

UV-A breakage sensitivity of human chromosomes as measured by COMET-FISH depends on gene density and not on the chromosome size

Alexander Rapp*, Claudia Bock, Heike Dittmar, Karl-Otto Greulich

Institut für Molekulare Biotechnologie, Postfach 100813, D-07708 Jena, Germany

Received 16 February 2000; accepted 9 April 2000

Abstract

COMET-FISH, a single cell-based combination of COMET-assay (also known as single cell gel electrophoresis (SCGE)) with fluorescence in situ hybridization (FISH) allows region specific studies on DNA stability and damage. COMET-FISH can be used to investigate UV-A-induced DNA damage of selected whole chromosomes. In the present work, a modified COMET-FISH protocol with whole chromosome painting probes was used to study whether UV-A-induced DNA damage is distributed randomly over the whole genome or occurs at preferred sites. The study was performed with 12 different chromosome painting probes (for chromosomes 1, 2, 3, 8, 9, 11, 14, 18, 19, 21, X and Y). The results on human lymphocytes irradiated with 500 kJ/m² at a wavelength of 365 nm indicate that the induced number of chromatin strand breaks does not correlate with the chromosome size. They therefore are distributed in a non-random manner. For example, fragments of the gene-rich chromosome 1 were found in the comet tail in only 3% of the examined cells, and thus chromosome 1 is rather stable, whereas fragmentation of the gene-poor chromosome 8 was observed in 25% of all comets. On the basis of all 12 chromosomes analyzed, an inverse correlation between the density of active genes and the sensitivity toward UV-A radiation is found. © 2000 Elsevier Science S.A. All rights reserved.

Keywords: DNA damage; COMET-FISH; COMET-assay; UV-A; Chromosome; Gene density

1. Introduction

Research on DNA damage induced by agents such as radiation, environmental toxins, DNA binding substances or therapeutics has been performed during the last years with the COMET-assay. This technique, first described by Östling and Johanson [1] in 1984 and in a modified version by Singh et al. [2] in 1988, allows easy and fast visualization and measurement of overall DNA damage on the level of the whole genome of single cells. The assay uses an electric field to separate damaged from undamaged DNA. Undamaged DNA is too large to move in the electric field and therefore remains in the place of the former nucleus. This part of the comet is termed the comet's head. On the other hand, damaged (fragmented) DNA is separated electrophoretically and generates the comet tail. Through the variation of lysis, electrophoresis buffers and electrophoresis conditions (variation of pH and ionic strength) different DNA damage such as single- or double-strand

breaks can be monitored [3–6]. For the present studies, we applied the alkaline version [2] of the COMET-assay which detects both, single- and double-strand breaks simultaneously. Comparison of the intensities of tail DNA and head DNA under a conventional fluorescence microscope allows quantification of the DNA damage, which can today be performed with automated software systems such as, e.g., Komet 4 (Kinetic Imaging, Liverpool) or VisComet (TILL-Photonics, Munich).

With the combination [7,8] of the COMET-assay and fluorescence in situ hybridization (for a review see Ref. [9]), termed COMET-FISH [10], specific genomic regions can be examined in the COMET-assay. For that, digoxigenin (DIG)-labelled probe DNA is added to the denatured comets. After hybridization, these probes are detected with fluorescence labelled anti-DIG-antibodies and therefore paint their corresponding sequence. Thus, specific sequences can be located in the head or the tail of the comet. By counting the ratio of cells with signals in the head and those with signals in the tail, the sensitivity of the specific genomic regions towards damaging agents can be calculated. In this way, this technique allows rapid and easy screening of DNA breakage sensitivity after exposure

*Corresponding author. Tel.: +49-3641-656-405; fax: +49-3641-656-410.

E-mail address: bar@imb-jena.de (A. Rapp).

to various kinds of damaging agents on the level of individual cells, and is a good tool to perform studies on region/locus specific DNA damage distribution in the human genome [11].

In the present work, we used COMET-FISH with 12 different whole chromosome painting probes to study whether UV-A (365 nm)-induced DNA damage is distributed randomly all over the genome or occurs at preferable sites. Similar studies for other kinds of radiation (e.g., UV-B and UV-C, and ionizing radiation [12–14]) have shown a non-random distribution of the DNA lesions. As the damaging mechanism of UV-A irradiation is known in molecular detail [15], these results could help to learn about the nuclear architecture [16] of chromosomes or chromosomal regions and how, for example DNA protein interaction or DNA conformation does influence the induced damage [17].

2. Experimental details

2.1. Cell preparation

Human lymphocytes, prepared from peripheral blood of three female and two male healthy donors with unsuspecting karyotypes were used in the experiments. Five ml blood were collected into tubes with 0.1% heparin solution. Lymphocytes used for COMET-FISH were isolated without previous incubation or cultivation. Three ml of lymphocyte separation medium (Gibco, Germany) were overlaid with 5 ml whole blood diluted 1:2 in 10 mM PBS (phosphate-buffered saline), pH 7.4, and then centrifuged at $200\times g$ for 30 min. The opaque layer with the monocytes was separated and diluted 1:2 in PBS and centrifuged as mentioned above, for 15 min. The supernatant was again centrifuged and the cells were resuspended in 400 μ l PBS. A cell concentration of 7.5×10^5 cells/ml was adjusted after counting in a Neubauer chamber.

2.2. Irradiation

The cells were irradiated with a 100-W high-pressure mercury lamp (HBO100; Zeiss, Germany). The 365-nm UV-A line was filtered by a bandpass of $\Delta\lambda=10$ nm (Zeiss, Germany) and focused into the cuvette with a focus diameter of 4 mm. The cells were irradiated in an ice-cooled cuvette under permanent stirring for 30 min. Stirring was performed in a 500- μ l self-made cuvette, placed directly on a magnetic stirrer, with 40 rpm. The radiation fluence of 500 kJ/m² on the sample was controlled with a power-meter (Sciencetech, Vektor 200, Laser2000, Germany). On the basis of dose–response curves determined in an early work [6,18], this fluence was chosen because of the clear biological effect with a considerable cell survival. To avoid heat damage, a heat

filter has been placed between the lamp and the probe cuvette.

2.3. COMET-assay and COMET-FISH

The variation of COMET-assay, as it was used in our experiments, was based on the alkaline COMET-assay described by Singh et al. [2]. This assay can detect single- and double-strand breaks by performing electrophoresis at high salt conditions and at pH over 13.

Frosted microscope-slides (Labcraft, UK) were pre-coated with 50 μ l of 1% normal melting agarose (Sigma, Germany) diluted in 0.01 M PBS followed by a second layer of 400 μ l normal melting agarose (1% diluted in 0.01 M PBS). Each layer was flattened with a coverslip until the agarose had turned solid. The irradiated cell suspension (7.5×10^5 cells/ml) was mixed with four volumes of low melting agarose (Sigma) (1% agarose diluted in distilled H₂O), to obtain a final agarose concentration of 0.8%. A volume of 60 μ l of the suspension was added to the previously prepared slides (see above) and again flattened using a coverslip. After the agarose was cooled down, the coverslip was removed and the slides were immersed in cold lysis buffer containing 2.5 M NaCl, 100 mM Na₂EDTA, 1% sodium sarcosinate, 1% Triton X-100, 10% DMSO and 10 mM Tris, pH 10, for at least 1 h at 4°C. The slides were drained and the cells were then treated in alkaline buffer (333 mM NaOH, 1 mM Na₂EDTA, pH 13) for 1 h at 4°C in order to denature the DNA. Electrophoresis was performed in fresh alkaline buffer for 35 min at 4°C and 1 V/cm. After neutralization in 0.5 M Tris, pH 7.5, for 5 min at room temperature, the slides have been stored in 98% ethanol at 4°C for up to 1 week.

Hybridization on cells embedded in agarose is mechanically critical, and should be handled carefully to avoid losing the agarose layers. Additionally, all solutions used for hybridization must be filtered through a 0.22- μ m membrane (Millipore, Germany) to avoid high background during fluorescence microscopy. The cellular DNA was first denatured in 0.5 M NaOH for 25 min at room temperature, drained and dehydrated by an increasing ethanol series (70%, 80% and 95%; 5 min each, at room temperature) and finally air dried. The digoxigenin-labelled probes were pre-denatured according to the protocol of the supplier (Oncor, Appligene) after concentrating the hybridization mixture with a spin column (Microcom 100; Millipore, Germany) the probe DNA was prehybridized at 37°C in the hybridization mixture (Hybrisol VI, Oncor, Appligene) for 15 min. Five to 60 μ l (optimized for each probe) of the pre-denatured DNA probe solution were added to the slides diluted with Hybrisol VI (Oncor, Appligene) making a final volume of 60 μ l. Afterwards, the slides were covered with plastic coverslips and incubated in a humidified chamber at 37°C for 12–72 h without sealing the slides. After hybridization the coverslips were carefully removed and the slides were washed in SSC (1 \times

to 2 \times , according to the probes protocol) at 70°C for 5 min and finally immersed in phosphate-buffered detergent (PBD). An enzyme coupled antibody (Boehringer Mannheim, Germany) [19] was used to enhance the fluorescence signal with HNPP/Fast Red as described by the supplier, except that the Fast Red solution was applied for just 10 min. The slides were washed for 10 min in H₂O and counterstained with diluted (1:100 in H₂O) SYBR Green solution (Molecular Probes) for 10 min in the dark.

After 30 min incubation at 4°C in the dark, image acquisition was performed using a fluorescence microscope (Axioskop; Zeiss, Germany) with a 40 \times /NA 1.33 oil immersion objective, appropriate filter sets (Zeiss), and a black and white CCD camera (Photometrix, USA). For image analysis the IPLab software was used running on a Macintosh computer. The fluorescence images of the comets, and the FISH-labelled sites are recorded separately as individual black and white images. Then the corresponding images were merged and presented in false colours. Quantitative analysis of the comet images was performed using Komet 3.0 (Kinetic Imaging) running on an IBM PC.

2.4. Variations in the appearance of comets and data analysis

Fig. 1 shows comets of different cells hybridized with a whole chromosome painting probe for chromosome 1 (upper row) and for chromosome 8 (lower row). For chromosome 1 the majority of the hybridization spots were localized in the comet's head. In contrast, for chromosome 8 a considerable number of hybridization signals was found in the tail. Since the irradiation dose and the electrophoretic conditions were equal for all nuclei, obviously chromosome 1 was more stable than chromosome 8. In order to quantify this, we have introduced a classification of the hybridization patterns according to Fig. 2: this figure also gives an estimate of fragment size versus position in the comet (see below). Grades 0 and 1 have no fragments smaller than ~100 kb and were defined as 'undamaged', although rare DNA breaks resulting in megabasepair sized fragments were still possible.

In a typical experiment, approximately 30–100 cells are evaluated per microscope slide. The number of cells counted depended on the quality of the gel matrix and the location of the comets. Sometimes comets were located close to each other, so that an evaluation was not possible. Also partly damaged gels (air bubbles included or scratched gels) reduce the numbers of comets that could be evaluated. The number of comets counted was not dependent on the probe, but differs from slide to slide. A typical COMET-assay or COMET-FISH experiment should consist of 50 or more cells per slide with three independently processed slides to get an overall minimum number of 150 cells to achieve statistical security. For chromosome 1, 194 comets (on four slides) were judged as class 0 and 1,

whereas six comets were class 2, resulting in an overall percentage of damaged cells of 3%. The corresponding values for chromosome 8 are 150 and 50 with a resulting percentage of 25%.

2.5. Estimation of fragment length

An estimate of fragment length as function of the position in the comet (Fig. 2, bottom) was obtained as follows: COMET-assay was performed as described above, except that the agarose concentration was varied from 0.5 to 5% and electrophoresis was carried out for 60 min. Parallel to this, normal agarose gels (also low melting point agarose) were loaded with a molecular size standard (Eurogentec) ranging from 200 to 10 000 basepairs. The electrophoresis was carried out in the same buffer and under the same electrophoretic conditions as described for the microgels.

The estimate of the fragments in the comet's tail was made from the comparison of the known DNA fragments and the comet's appearance. It is known, that DNA larger than 100 kb cannot enter even low concentrated agarose gels [20]. These fragments must remain in the head. The fragments from 10 to 100 kb can migrate in low concentrated, but not in higher concentrated agarose, that results in normal comets in low concentration agarose microgels. However fragments smaller than 10 kb migrate also in high concentrated gel matrix. This results in a normal separated standard in the macroscopic gel and comet's with a 'broken tail', that means the smallest fragments of the comets tail are completely separated from the head, so that the middle part of the tail is missing. These medium sized fragments are missing in the comets in 2.5% agarose for example. The smallest fragments in the comets are small enough to migrate in agarose up to 4%, whereas in the macroscopic gels at 4–5% fragments over 8000–10 000 bp do not migrate. So the estimation is build on the observation of the missing fragments in the comets and the corresponding standard fragments, that could not migrate into the macroscopic gels.

2.6. Controls using metaphase chromosome spreads and laser scanning microscopy (LSM) analysis

For all tested probes, hybridization on metaphase spreads was performed before the probes were used in COMET-FISH to check their quality, stringency and the optimal hybridization conditions. The hybridization on metaphase chromosomes was performed according to standard cytogenetic protocols on methanol acetic acid fixed chromosomes and nuclei [21].

Control experiments for COMET-assay were performed with undamaged cells, that were passed through lysis and electrophoresis without previous damaging. Also cells were stirred in the micro-cuvette for 30 min without irradiation on ice and without any detectable DNA dam-

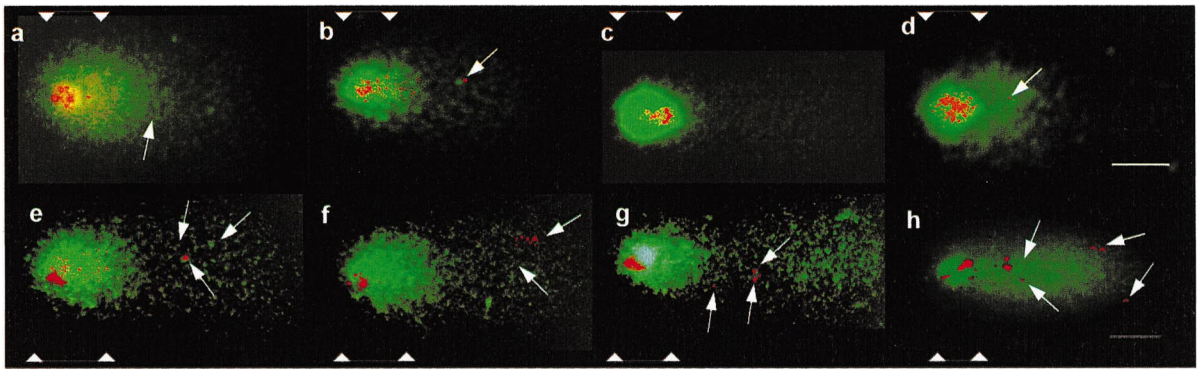


Fig. 1.

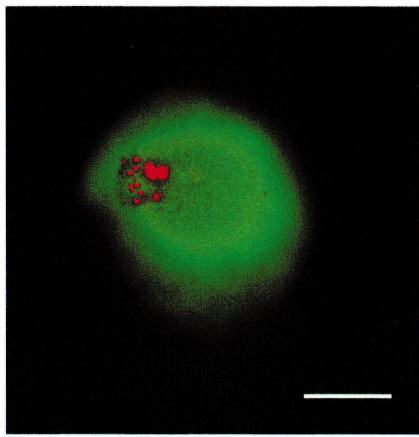


Fig. 3.

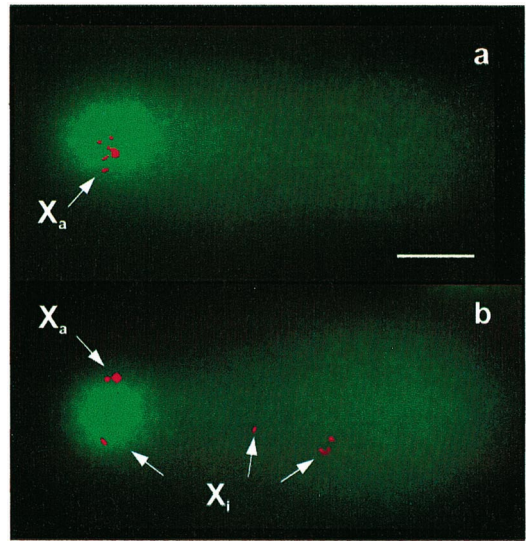


Fig. 5.

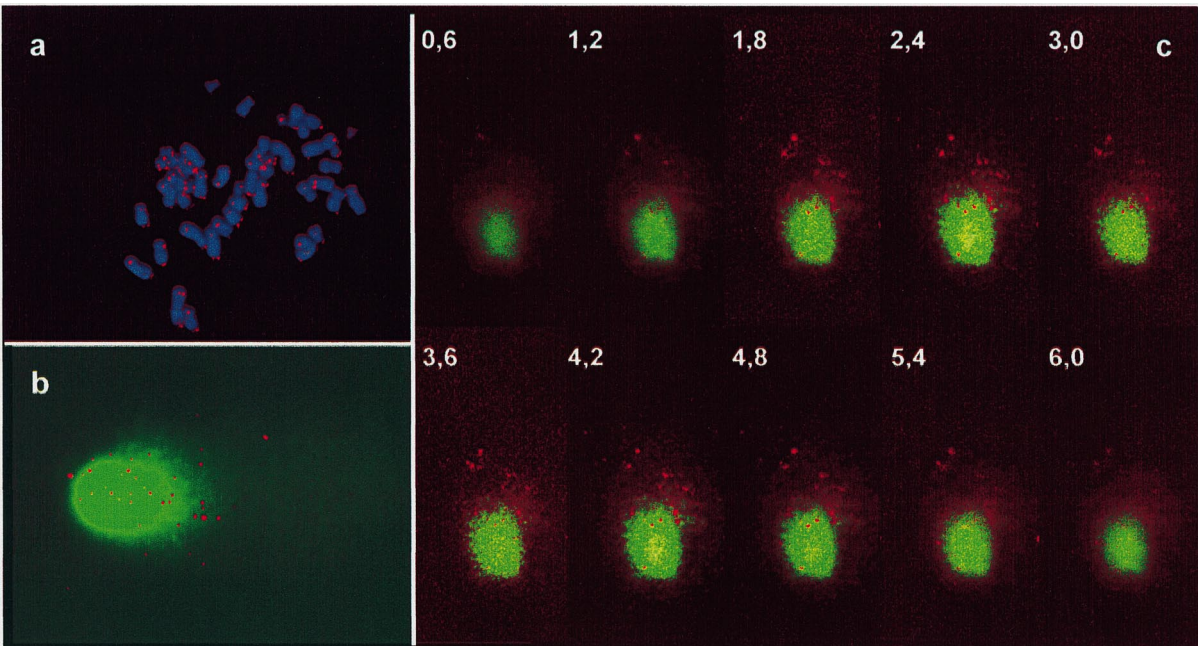


Fig. 4.

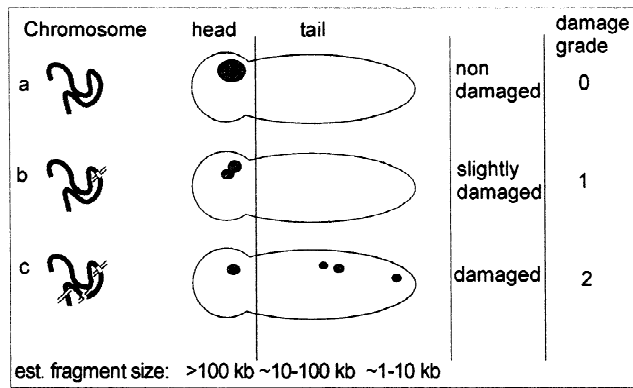


Fig. 2. Schematic overview of possible breakage patterns and the resulting hybridization signal distribution after COMET-FISH. Case (a) represents a completely undamaged chromosome, which results in only one signal in the head. This case would be correctly judged as 'undamaged'. Case (b) shows a low level fragmentation, which results in large unmovable fragments that form a fragmented cluster in the head. This case will be judged as undamaged, whereas it is slightly damaged. Case (c) shows a damaged chromosome with signals clustered in the tail. This pattern would be correctly interpreted as 'damaged'. An estimate of the fragment size is given at the bottom of the illustration.

age. The comets of these nuclei kept their round shape, i.e., no DNA fragments migrated out of the nucleus. An image of a control (male) nuclei is presented in Fig. 3, hybridized with a whole chromosome painting probe for chromosome X. No damaged DNA was found, that migrates out of the head. The hybridization reveals one distinct chromosomal domain known from interphase FISH.

Hybridization on comets and unirradiated control nuclei embedded in agarose was controlled by three-dimensional LSM to ensure that hybridization signals were located in the comet volume and have the expected spatial dimensions. For these experiments a Zeiss LSM 510, equipped with a helium–neon and an argon ion laser, was used. Images were acquired with a pinhole diameter of 1.04 Airy units and an adequate amplification gain to get the optimum signal-to-noise ratio. The comets were visualized at 1024×1024 pixels using the Zeiss LSM software

version 2.04. The sections in z -direction were captured at a distance of $0.6 \mu\text{m}$ as suggested by the software. Hybridization patterns of multiple probes as 'all-human-centromere' or telomere probes were compared between COMET-FISH and metaphase chromosome hybridization (see Fig. 4).

2.7. Expressed sequence tags (EST) and EST-density

An EST is an arbitrary piece of DNA sequence in the (human) genome which is a result as well as a working tool for large genome sequencing projects such as HUGO. Typically, one obtains ESTs by isolating messenger RNA of a given cell (type), reverse-translating it into cDNA and determining a part of its sequence, up to a few hundred basepairs long. The EST information is gathered in data bases (for an overview, see Ref. [22]). EST-specific data are available in these data bases, for example the position of each EST on a chromosome or disease related data. Over the past years, sufficient information on ESTs has accumulated to generate a map of ESTs for each chromosome. Since ESTs have been generated from mRNA, i.e., expressed RNA, the density of ESTs on a given chromosome is related to the density of active (expressed) genes. To correlate the measured breakage sensitivity to the gene density, the density of active genes for each chromosome is given as the EST density. These densities are calculated by chromosome mapping researchers after allocation of thousands of cDNA clones. The EST density is calculated as given in Eq. (1):

$$\text{EST}_{\text{density}} = \frac{N_{\text{counted}}}{N_{\text{total}} \times \frac{\text{DNA}_{\text{chromosome}}}{\text{DNA}_{\text{genome}}}} \quad (1)$$

with N_{counted} is the number of clones allocated to a specific chromosome, and N_{total} is the overall number of tested or localized clones. $\text{DNA}_{\text{chromosome}}$ means the DNA content of the specific chromosome, while $\text{DNA}_{\text{genome}}$ means the total DNA content of all chromosomes of the specific

Fig. 1. Typical results of two hybridization probes used in COMET-FISH after 500 kJ/m^2 UV-A irradiation. These images show the variation among individual cells of the resulting hybridization patterns, as discussed in previous sections. Upper row (a–d): typical results of the 'stable' chromosome 1. Lower row (e–h): chromosome 8, that is less stable. The white triangles indicate the head dimensions as calculated by the computer software Komet 3.0. The white scale bar represents a distance of $10 \mu\text{m}$. The arrows show the location of the small hybridization signals in the comets.

Fig. 3. Control nucleus of a male donor: the cell was passed through the complete preparation procedure, except that it was not irradiated. There was no detectable DNA damage. The hybridization pattern of a whole chromosome painting probe of chromosome X reveals a distinct chromosomal domain. The white scale bar represents a distance of $10 \mu\text{m}$.

Fig. 4. All human telomere probe hybridized on (a) spread human metaphase chromosomes, (b) hybridization on a comet observed with an epifluorescence microscope (c), and gel embedded comet, displayed as a z -stack acquired with a LSM. Similar numbers of signals and signal intensities were observed with all three methods.

Fig. 5. In contrast to Fig. 1, the pattern of the X chromosome specific probe of a male (a) and female (b) donor. In the latter case, one signal cluster can be found in the tail, indicating comparably high radiation sensitivity, whereas the second signal can be found in the head area in nearly all cases. (A) The same probe as (b) except that in this case the cells of a male donor are taken, showing significant differences in the stability of the X chromosome in male and female donors, with one major signal cluster in the head and rarely signals in the tail. The white scale bar is $10 \mu\text{m}$. The arrows locate the small hybridization signals in the comets.

Table 1

An overview of the FISH probes used in COMET-FISH^a

Probe	Metaphase			COMET-FISH			
	No. experiments	No. spreads	% Hybridization ^b	No. experiments	No. nuclei	No. signals	% Hybridization ^b
1	1	100	98	4	200	2	92
2	1	100	97	1	80	2	94
3	1	100	98	1	75	2	90
8	1	100	99	4	200	2	91
9	1	100	97	2	80	2	94
11	1	100	100	2	90	2	90
14	1	100	100	2	70	2	93
18	1	100	98	1	65	2	95
19	1	100	99	2	130	2	95
21	1	100	98	4	100	2	89
X male	1	100	97	4	180	1 signal	90
X female	1	100	98	5	200	2 signals	85
Y	1	100	97	4	180	1	92
All centromeres	2	200	91 (>70 sign.)	4	160	60–70	82
All telomeres	2	200	82 (>42 sign.)	4	160	36–46	81

^a The first three columns show the results of control experiments on metaphase chromosome spreads.

^b % Hybridization means the number of objects (metaphases or interphase nuclei) with the expected results. The expected results are given in the column 'No. signals'. The last four columns represent the results of the COMET-FISH experiments. The percent of signals in the tail means one or two signals in the tail (see text for explanation), whereas the No. signals indicates the expected number of signals to be found.

genome. The EST density is calculated by dividing the counted clone probes mapped on a specific chromosome by the product of the total number of tested cDNA clones and the percentual chromosome size. A value smaller than 1 indicates a chromosome with a gene density below the average, whereas values above 1 indicate gene-rich chromosomes.

2.8. Error calculations

Error bars shown in Fig. 6, and also listed in Table 2, were calculated as follows: the percentage of nuclei with signals in the tail was calculated for each slide. The numbers of experiments per probe are given in Table 1. The total percentage of comets with signals in the tail was calculated as percentage averaged from the single experiments per probe. The errors were determined by the standard deviations (for some probes only one experiment was performed, so no error was calculated). The EST density for each chromosome was the averaged value obtained from the two publications of Hudson and co-workers [23] and Deloukas and co-workers [24]. The error bars were also calculated as the standard deviation.

3. Results

3.1. Comparison of hybridization on COMETS versus hybridization on metaphase chromosomes

Fig. 4 shows the result of in situ hybridization on

metaphase chromosomes and on comets. Fig. 4a gives the result of an 'all human telomere' probe hybridized on a metaphase spread. Comparable results are obtained when the probe is hybridized on comets, with similar number of signals and similar signal size. To ensure complete detection, Fig. 4b gives the z-stack obtained by LSM observation of an acquired comet in comparison to Fig. 4c, which shows a comet with the same hybridization probe observed in a conventional epifluorescence microscope. So COMET-FISH gives comparable results with respect to hybridization sensitivity and reproducibility as conventional metaphase hybridization. Conventional microscopy can be used for routine measurements, while LSM may be applied to obtain high resolution comets for hybridization control. With the described protocol, especially chromosome painting probes can be hybridized successfully and analyzed.

3.2. UV-A sensitivity of whole chromosomes

From the distribution of the whole chromosome painting FISH signals in the comet tail or head, a correlation of damaged versus undamaged DNA in the respective chromosome can be evaluated. COMET-FISH can detect all DNA breaks (single or double strand) that exceed a given detection limit, defined by the minimum size of the fragments that can be separated from the unfragmented DNA within the electric field. As this limit is similar for all DNA fragments from all chromosomes, the counted cases can be correlated to an induced number of breaks. As an example, the image of COMET-FISH for a chromosome 1

Table 2

Overview of the tested chromosomes together with the DNA content in megabasepairs^a

Chromosome	% Cases with signals in tail	Standard error	Mean EST density	DNA content in Mb
1	3	2.62	1.32	250
2	8.1	0 ^b	0.865	240
3	8.9	0 ^b	0.945	190
8	25	4.42	0.76	135
9	7	1.5	1	130
11	2	1	1.39	130
14	2	1.75	1.19	105
18	10.9	0 ^b	0.675	75
19	2	1	2.17	70
21	6	3.53	0.81	55
X	18	3.80	0.58	140
Y	30	7.59	n.a.	60
X _{female}	93	4.39	0.58	140

^a A random distribution of induced UV-A breaks should result in more cases with signals in the tail for large chromosomes than for small ones. The ratio of observed breaks for each chromosome and the chromosomes corresponding mean EST density as known from literature (see text). Also the standard deviation for the observed cases with breaks is given, as calculated from the results of the single experiments.

^b For these data no standard deviations could be calculated, as these experiments were only performed once. n.a. (not assigned): The EST value is not given in the literature.

painting probe is shown in Fig. 1 upper row. The labelled sites are nearly always located in the head, showing the typical shape of chromosome territories known from interphase FISH [25,26] on standard microscope slides. On the contrary, Fig. 1 lower row shows the result of hybridization of chromosome 8, that reveals significantly more comets with signals in the tail. Similar results as for chromosome 1 are obtained with the DNA painting probes for chromosomes 11, 14 and 19 (see Table 2). A second class of chromosomes consists of a group with intermediate chromosome fragility where a few chromosome signals are found in the tail in 6–10% of the comets (these are chromosomes 2, 3, 9, 18 and 21). In contrast to these chromosomes, chromosomes 8, X and Y (18–30%) show more signals in the tail (Table 2).

The X chromosome reveals a sex-specific behaviour for all tested individuals: 93% of the comets show FISH signals in the tail for *female nuclei* (Fig. 5b), but only 18% of *male nuclei* do so (Fig. 5a), suggesting that it may be the inactive X chromosome (X_i), which is heavily damaged.

3.3. Chromosome fragility versus DNA content and EST density

The sensitivities for all tested chromosomes are listed in Table 2, together with the DNA content in megabasepairs. If the UV-A induced damage would be distributed randomly, there should be a linear correlation between DNA content of the chromosomes and their sensitivity towards UV-A irradiation. Therefore, the larger chromosomes (1, 2

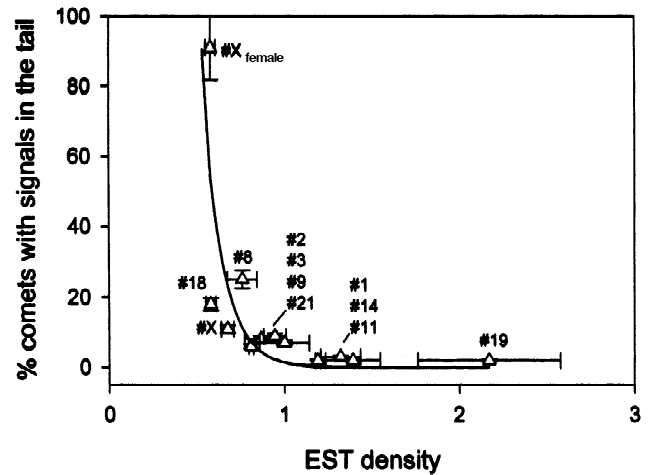


Fig. 6. DNA breakage sensitivity, expressed as the percentage of comets with signals in the comet tail as function of the gene density, depicted as expressed sequence tags (ESTs) for the chromosomes (Δ). The data are fitted by an exponential function (—). Error bars for the EST values are calculated as the standard deviation from the different EST values given in the cited articles. Error bars for the percentage of cases with signals in the tail are calculated as the standard deviation from the results of the single experiments for the breakage sensitivity. An inverse correlation between the gene density and the breakage sensitivity is displayed.

and 3) should have a higher number of DNA breaks than the smaller ones (chromosomes 19 and 21). We did not find such a correlation between DNA content and the number of UV-A induced breaks. This means that DNA damage seems not to be induced in a random or size depended way, but at some preferred sites or ‘hotspots’.

The behaviour of the female sex chromosomes, compared to that in male nuclei implicates another correlation. The breakage sensitivity seems to be correlated to the density of active genes. A good measurement for the density of active genes is the density of mapped expressed sequence tags (ESTs, see <http://www.ncbi.nlm.nih.gov/genemap/>). The breakage sensitivities for all tested chromosomes have been correlated to the corresponding mean EST densities published by Hudson and co-workers [23] and Deloukas and co-workers [24]. The correlation is given in Fig. 6. An empirical fit function is shown based on an exponential function. Any biological meaning, however, is presently not obvious, so that this exponential decrease should only be used as an empirical fact.

4. Discussion

So far the published protocols of FISH on comets [10,11] have only used ‘small’ hybridization probes, whereas the modified protocol for COMET-FISH [9,10] described in this paper is appropriate to perform hybridization with whole chromosome painting probes as well. This makes COMET-FISH a fast and easy method to study stabilities of specific chromosomes towards DNA damage.

ing agents. The described protocol achieves sensitivity and stringency comparable to hybridization on metaphase or interphase chromosomes. Hybridization time, probe concentration and gel thickness are critical, among them the most critical one is the top layer thickness, which in addition strongly affects the optical properties of the gel sandwich, since thinner layers result in a better signal detection and less background or scattering.

Attempts to find a correlation between the chromosome size or its DNA content and the number of UV-A-induced breaks were inconclusive. Even a statistic random distribution could not be found. Since UV-A induces DNA damage in a different way from ionizing radiation, a direct extrapolation from former findings of UV-C and ionization induced damage was not feasible. This damage were reported to occur in a non-random manner [14,27,28]. Chromosome structure, genomic imprinting or the localized activity of repair enzymes were mentioned as possible causes for the unequal distribution of DNA damage [29,30].

However, we have found a completely different, size-independent, correlation. DNA breakage sensitivity is correlated with the density of active genes, given as the density of expressed sequence tags (ESTs). The data show an inverse relationship between the gene density and the UV-A sensitivity, since gene poor chromosomes seem to be more damaged than gene rich ones. For example, the highly sensitive X chromosome in female nuclei is probably the inactive X (X_1), which has a low density of active genes. On the other hand, chromosomes 1 and 19, which have a high density of active genes (high EST densities) show a low sensitivity towards UV-A. The other tested chromosomes also fit this theory resulting in Fig. 6 and the calculated fit function. On the contrary, X-ray induced DNA damage occurs preferably in gene rich regions [12,13,31], indicating a different overall damaging mechanism.

As is known, gene-poor genomic regions have a lower repair enzyme activity [32]. This may be a possible explanation for the unequal distribution of the measured DNA breaks. A working hypothesis is that the higher repair enzyme activity located at active gene loci [32] is capable of repairing UV-A-induced DNA damage so fast [33,34] that these regions show an overall reduced damage. This repair activity has been reported to occur also at 4°C [33], so that DNA damages could be repaired during irradiation and within the 5 min between irradiation and lysis. Nevertheless, further research has to be done to clarify whether enzyme activity alone or chromosome structure and enzyme activity led to the reduced sensitivity of active gene regions towards UV-A irradiation.

Acknowledgements

This work was supported by the Fonds der Chemischen Industrie grant 161971.

References

- [1] O. Östling, K.J. Johanson, Microelectrophoretic study of radiation-induced DNA damages in individual cells, *Biochem. Biophys. Res. Commun.* 123 (1984) 291–298.
- [2] N.P. Singh, M.T. McCoy, R.R. Tice, E.L. Schneider, A simple technique for quantitation of low levels of DNA damage in individual cells, *Exp. Cell Res.* 175 (1988) 184–191.
- [3] V.J. McKelvey-Martin, M.H. Green, P. Schmezer, B.L. Pool-Zobel, M.P. De Meo, A. Collins, The single cell gel electrophoresis assay (comet assay): a European review, *Mutat. Res.* 288 (1993) 47–63.
- [4] D.W. Fairbairn, P.L. Olive, K.L. O'Neill, The comet assay: a comprehensive review, *Mutat. Res.* 339 (1995) 37–59.
- [5] M. Klaude, S. Eriksson, J. Nygren, G. Ahnstrom, The comet assay: mechanisms and technical considerations, *Mutat. Res.* 363 (1996) 89–96.
- [6] A. de With, G. Leitz, K.O. Greulich, UV-B-laser-induced DNA damage in lymphocytes observed by single-cell gel electrophoresis, *J. Photochem. Photobiol. B* 24 (1994) 47–53.
- [7] S.J. Santos, N.P. Singh, A.T. Natarajan, Fluorescence in situ hybridization with comets, *Exp. Cell Res.* 232 (1997) 407–411.
- [8] V.J. McKelvey-Martin, E.T. Ho, S.R. McKeown, S.R. Johnston, P.J. McCarthy, N.F. Rajab, Emerging applications of the single cell gel electrophoresis (Comet) assay I. Management of invasive transitional cell human bladder carcinoma. II. Fluorescent in situ hybridization comets for the identification of damaged and repaired DNA sequences in individual cells, *Mutagenesis* 13 (1998) 1–8.
- [9] P. Lichter, Multicolor FISHing: what's the catch?, *Trends Genet.* 13 (1997) 475–479.
- [10] C. Bock, S. Monajembashi, A. Rapp, H. Dittmar, K.O. Greulich, Localisation of specific sequences and DNA single strand breaks in individual UV-A irradiated human lymphocytes observed by COMET FISH, *Proc. SPIE* 3568 (1999) 207–217.
- [11] A. Rapp, C. Bock, H. Dittmar, K.O. Greulich, COMET-FISH used to detect UV-A sensitive regions in the whole human genome and on chromosome 8, *Neoplasma* 46 (Suppl.) (1999) 99–101.
- [12] P. Slijepcevic, A.T. Natarajan, Distribution of X-ray-induced G2 chromatid damage among Chinese hamster chromosomes: influence of chromatin conformation, *Mutat. Res.* 323 (1994) 113–119.
- [13] P. Slijepcevic, A.T. Natarajan, Distribution of radiation-induced G1 exchange and terminal deletion breakpoints in Chinese hamster chromosomes as detected by G banding, *Int. J. Radiat. Biol.* 66 (1994) 747–755.
- [14] K.L. Johnson, D.J. Brenner, J. Nath, J.D. Tucker, C.R. Geard, Radiation-induced breakpoint misjoining in human chromosomes: random or non random, *Int. J. Radiat. Biol.* 75 (1999) 131–141.
- [15] F. Greiter, F. Gschnait, Effect of UV light on humans, *Photochem. Photobiol.* 39 (1984) 869–873.
- [16] C. Cremer, T. Cremer, C. Zorn, L. Schoeller, Effects of laser UV-microirradiation ($\lambda = 2573 \text{ \AA}$) on proliferation of Chinese hamster cells, *Radiat. Res.* 66 (1976) 106–121.
- [17] L.H. Mullenders, A.C. Van Kesteren van Leeuwen, A.A. van Zeeland, A.T. Natarajan, Nuclear matrix associated DNA is preferentially repaired in normal human fibroblasts, exposed to a low dose of ultraviolet light but not in Cockayne's syndrome fibroblasts, *Nucleic Acids Res.* 16 (1988) 10607–10622.
- [18] A. de With, K.O. Greulich, Wavelength dependence of laser-induced DNA damage in lymphocytes observed by single-cell gel electrophoresis, *J. Photochem. Photobiol. B* 30 (1995) 71–76.
- [19] N. Kagiya, K. Yoshida, T. Hamabata, N. Juni, T. Awasaki, S. Fujita, M. Momiyama, M.C. Yoshida, S.H. Hori, A novel fluorescent method for in situ hybridization, *Acta Histochem. Cytochem.* 26 (1993) 441–445.
- [20] R. Martin, in: *Gel Electrophoresis: Nucleic Acids*, Bios Scientific Publishers, Oxford, UK, 1996.
- [21] Methods in molecular biology, in: K.H.A. Choo (Ed.), *In Situ Hybridization Protocols*, Vol. 33, Humana Press, Totowa, 1994.
- [22] R.L. Strausberg, K.H. Buetow, M.R. Emmert-Buck, R.D. Klausner,

- The Cancer Genome Anatomy Project: building an annotated gene index, *Trends Genet.* 16 (2000) 103–106.
- [23] T.J. Hudson, L.D. Stein, S.S. Gerety, J. Ma, A.B. Castle, J. Silva, D.K. Slonim, R. Baptista, L. Kruglyak, S.H. Xu et al., An STS-based map of the human genome, *Science* 270 (1995) 1945–1954.
- [24] P. Deloukas, G.D. Schuler, G. Gyapay, E.M. Beasley, C. Soderlund, P. Rodriguez-Tome, L. Hui, T.C. Matise, K.B. McKusick, J.S. Beckmann et al., A physical map of 30,000 human genes, *Science* 282 (1998) 744–746.
- [25] R. Eils, E. Bertin, K. Saracoglu, B. Rinke, E. Schrock, F. Parazza, Y. Usson, M. Robert-Nicoud, E.H. Stelzer, J.M. Chassery et al., Application of confocal laser microscopy and three-dimensional Voronoi diagrams for volume and surface estimates of interphase chromosomes, *J. Microsc.* 177 (1995) 150–161.
- [26] D. Zink, H. Bornfleth, A. Visser, C. Cremer, T. Cremer, Organization of early and late replicating DNA in human chromosome territories, *Exp. Cell Res.* 247 (1999) 176–188.
- [27] C. Cremer, C.H. Munkel, M. Granow, A. Jauch, S. Dietzel, R. Eils, X.Y. Guan, J.M. Meltzer, J. Lanowski, T. Cremer, Nuclear architecture and the induction of chromosomal aberrations, *Mutat. Res.* 366 (1996) 97–116.
- [28] E. Sage, Distribution and repair of photolesions in DNA: genetic consequences and the role of sequence context, *Photochem. Photobiol.* 57 (1993) 163–174.
- [29] G.L. Diculescu, The sources of variation in the human genome and genome instability in human cancers, *Rom. J. Physiol.* 34 (1997) 3–17.
- [30] A.P. Wolffe, Inheritance of chromatin states, *Dev. Genet.* 15 (1994) 463–470.
- [31] J.D. Tucker, J.R. Senft, Analysis of naturally occurring and radiation-induced breakpoint locations in human chromosomes 1, 2 and 4, *Radiat. Res.* 140 (1994) 31–36.
- [32] E.C. Friedberg, Relationships between DNA repair and transcription, *Annu. Rev. Biochem.* 65 (1996) 15–42.
- [33] C. Bock, H. Dittmar, H. Gemeinhardt, E. Bauer, K.O. Greulich, Comet assay detects cold repair of UV-A damages in a human B-lymphoblast cell line, *Mutat. Res.* 408 (1998) 111–120.
- [34] O. Kleinau, F. Bohm, B. Lanto, Different DNA repair time courses in human lymphoid cells after UVA, UVA1, UVB and PUVA in vitro, *J. Photochem. Photobiol. B* 41 (1997) 103–108.